ISSN (Print 0974-2115) (Online 2349-8552)
www.jchps.com Journal of Chemical and Pharmaceutical Sciences

Photocatalytic degradation of Methylene Blue by Biogenic Ag-Cu Bimetallic Nanoparticles

Ravi Chandra Gurrala[1], J. Prem Chand[1], M. Padma[1], N. Annapurna[1], S. Aruna Kumari[3], Ch. Jogi Narayana[1], B. Swarna Latha[2], Kishore Babu Bonige[1]*

[1]Department of Engineering Chemistry, Andhra University, Visakhapatnam.
[2]Department of Physics and Engineering Physics, Andhra University, Visakhapatnam
[3]Department of Chemistry, Aditya Engg College, Surampalem

***Corresponding Author: E-Mail ID: jacobkishore@gmail.com**

ABSTRACT

Using *Croton blanpondinum* L leaf extract, an ecologically acceptable and cost-effective approach for green production of Ag-Cu bimetallic nanoparticles was described. For the biosynthesized nanoparticles, the Phyto compounds contained in the extract operate as reducing, stabilizing, and capping agents. UV-VIS, FTIR, EDX, and XRD spectroscopies were used to characterize the samples. These nanoparticles were also used as photocatalysts to degrade Methylene Blue dye when exposed to sunshine. The best conditions for the degradation of malachite green dye were determined in this work on bimetallic Ag-Cu nanoparticles produced from *Croton blanpondinum* L leaf extract: pH 8, weight of catalyst 30 mg, dye concentration 10 ppm, and contact period 180 minutes. A maximum photo-degradation of ~ 85-89% could be obtained under these optimum conditions.

KEY WORDS: Bimetallic nanoparticles (BMNPs), *Croton blanpondinum L* (CB), Methylene Blue (MB), photo degradation.

1. INTRODUCTION

Nanotechnology is one of the most fascinating fields in science, with nanotechnology receiving the bulk of the ongoing debates, definitions, and research focus. Nanotechnology is a subset of technology that encompasses the study of nanoscale phenomena and may be found in colloidal science, chemistry, physics, biology, and other scientific disciplines (Mansoori and Soelaiman, 2005). Nanotechnology is defined as any technology that operates on the nanoscale (1-100nm) and has real-world applications, such as using single atoms and molecules to build functional structures (Kaehler, 1994). The study and use of chemical, physical, and biological systems with structural features ranging from single atoms or molecules to sub-micron dimensions, as well as the integration of the resulting nanostructures into real-world systems, is known as nanotechnology (Daniel and Astruc, 2004). Bimetallic nanoparticles have recently received a lot of interest due to their usefulness in magnetic, optical, and catalytic applications in a variety of domains (Venkatesan and Santhanalakshmi, 2011; Srinoi, 2018). For the synthesis of nanomaterials, there are a variety of approaches that may be used. Chemical techniques are commonly employed for nanomaterial production because they need less time and can produce large quantities of nanomaterials. Furthermore, chemical reagents usually utilised for nanoparticle production and stabilisation are toxic and can result in dangerous by-products that are not ecologically friendly (Pantidos, 2014; Shah, 2015). The desire for environmentally benign, non-hazardous nanomaterial synthesis processes is rising, as is the demand for biosynthetic procedures that do not entail the consumption of harmful chemicals as by-products. Plants, algae, actinomyces, yeast, bacteria, and fungus, among other natural sources, are used to synthesise metal nanomaterials (Park, 2011). Bio-mediated synthesis of noble nanometals (Au, Pt, and Ag nanoparticles) utilising fungus, bacteria, algae, and also from various sections of plants such as roots, leaves, flowers, stems, and so on has grown in importance as a safe alternative to physical and chemical operations (Lee, 2014).

Plant extracts are used to make nanomaterials, which is a cost-effective, environmentally friendly, and simple process. As a result, it may be employed as a cost-effective and beneficial alternative for the synthesis of metal nanoparticles. The bio reduction of metals using combinations of phytomolecules found in plant extracts such as phenols, amides, sterols, flavonoids, terpenoids, carbohydrates, and amino acids is a green technique that is ecologically friendly (Koduru, 2018; Maksakova, 2020; Greer and Nix, 2006).

South Western Brazil, Northern Argentina, Paraguay, Southern Bolivia, and India are all home to *Croton bonplandianum* L. Bana Tulasi or Kala Bhangra is a tiny annual plant that belongs to the Euphorbiaceae family. As reported, *Croton bonplandianum* L has several medicinal usages and also shows insect repellent properties (Jeeshna, 2011), *Croton bonplandianum L* was also show stabilizing to exhibit antibacterial (Parthiban, 2021), antifungal, antioxidant (Divya, 2011), analgesic (Sahoo, 2010), nematicide, anticoronary (Chandel, 2011), hepatoprotective, and wound healing properties (Sirdeshpande, 2018).

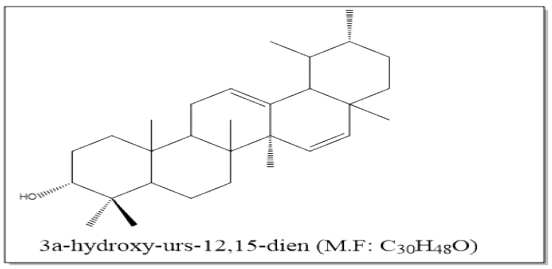

Figure.1. Major Chemical constituent identified in *Croton bonplandianum L* leaves

Methylene blue is a chloride salt of organic methylene with the formula $C_{16}H_{18}Cl\ N_3S$. It's also known as Swiss Blue or Methylthioninium chloride.

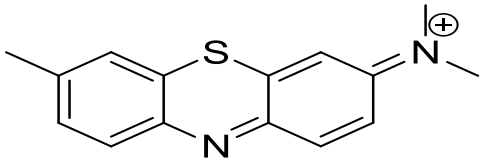

Figure.2. Methylene blue

It's a thiazine dye with antioxidant, cardiovascular, antimalarial, and depressive properties. Methemoglobinemia can occur when a person is exposed to certain drugs or chemicals, such as nitrates. Methylene blue injection is used to treat methemoglobinemia. By converting methemoglobin into a more effective type of haemoglobin, methylene blue aids in the storage of oxygen in the body. Side effects include headaches, vomiting, high blood pressure, disorientation, allergic reactions, and shortness of breath, red blood cell disintegration, and serotonin syndrome. The color of urine, feces, and sweat changes from blue to green as a result of this. This enzyme converts ferric iron in haemoglobin to ferrous iron.

Isosulphan blue/patent blue V in conjunction with a radioactive colloid tracer is a widely used method. MB is a less costly and more widely available alternative dye. The dye and radioisotope were injected into the subdermall plane in the subareolar area. Under UV irradiation, methylene blue dye (MB) was photo catalytically destroyed in an aqueous solution employing Ag-Cu bimetallic nanoparticles.

In the breakdown of methylene blue in wastewater, several techniques have been used solely, including biological treatment, ozonation, incineration, and adsorption on particles. These methods, on the other hand, produce toxic by-products and need lengthy routes. Heterogeneous photocatalysis is a less harmful approach for dye degradation that can provide harmless end products (Lakshi Saikia, 2015; Ravindra Kumar Gautam, 2015).

The effective photo-degradation of organic dye requires the identification of optimal process parameters. pH, initial pollutant/substrate concentrations, catalyst loading, temperature, and irradiation light intensity are all critical factors (Ramamurthy, 2013). BMNPs' optical characteristics are critical for their effective photocatalytic activity.

The use of leaf extract of *Croton blanpondinum* L as a stabilizing, reducing, and capping agent in the synthesis of Ag-Cu bimetallic nanoparticles (BMNPs) was reported here, and the use of these BMNPs as catalysts for photo-degradation of MB dye carried out under UV light irradiation was also studied at various reaction conditions to determine the optimum conditions for maximum photo-degradation.

2. EXPERIMENTAL

Materials: Chemical reagents used (silver nitrate ($AgNO_3$), nickel nitrate ($Cu(NO_3)_2$), ammonium hydroxide (NH_4OH) and Hydrochloric Acid (HCl), Ethanol, 1% HCl, Mayer's reagent, Dragendoff's reagent, Wagner's reagent, magnesium ribbon, 2% solution of NaOH, glacial acetic acid, $FeCl_3$, concentrated H_2SO_4, chloroform, gelatin solution, lead tetra acetate, bromine water, lead sub acetate, benedict's reagent, molisch's reagent, Millon's reagent, 0.2% solution of ninhydrin, 2% copper sulfate solution, potassium hydroxide, acetic anhydride. In this study all chemicals used were of analytical grade. Deionized water was used to clean glassware, to prepare chemical solutions and for experimental procedure. Fresh leaves of *Croton bonplandianum* L was collected from the barren lands in and around Lakshmipuram village in Jeelugumelli Mandal of West Godavari district in the Andhra Pradesh state of India, where it was found naturally.

Preparation of leaf extract: The leaves were separated from the branches and washed properly under running piped water two times to remove dust, debris, and other impurities and then with double distilled water two times. Now, these leaves were made to dry under shade for 7 days and these leaves were sliced into tiny pieces and made powder by using the home blender. The obtained powder was kept in an airtight container at 4^{o}c in a refrigerator for further usage (Selvamangai and Anusha Bhaskar, 2012). Collections were made in the mornings during the days of each analysis (Oyi, 2010).

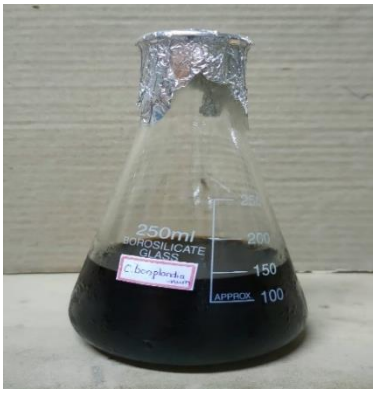

Figure.3. Leaf Extract *Croton bonplandianum L*

Synthesis of Ag-Cu bimetallic nanoparticles: $AgNO_3$ solution was prepared by dissolving 1.6987 g (10mM) of $AgNO_3$ and 100 ml of distilled water in a 500 mL beaker. And $Cu(NO_3)_2.3H_2O$ aqueous solution was prepared separately by dissolving 3.0079 g (10mM) of $Cu(NO_3)_2.3H_2O$ in 100 mL distilled water. To the 80 mL of above prepared and filtered green aqueous leaf extract of *C. bonplandianum L was added to the* aqueous solution of silver nitrate. Then reaction mixture turned in to pale brown color. And to the separately prepared 100 mL of $Cu(NO_3)_2.3H_2O$ solution were added drop wise in the simultaneous addition process. After this addition, the beaker was placed on a magnetic stirrer for continuous agitation and the mixture was stirred at 80^0C for 90 minutes at pH 8. The pH of the reaction medium could be adjusted by adding an adequate amount of 0.1 N HCl or 0.1 N NH_4OH solutions. After 90 minutes the color of the reaction mixture is turned into dark brown color it conforms to the formation of the Ag-Cu bimetallic nanoparticles. These synthesized BMNPs were separated out by doing centrifugation at 5000 rpm for 50 minutes. The obtained BMNPs were washed with deionized water three times to remove unwanted constituents and dried in an oven at 70^0C for three hours. The resultant Ag-Cu BMNPs particles were collected and used to further characterization.

Figure.4. Preparation of Ag-Cu BMNPs from precursor solutions

Phytochemical Screening of Leaf Extract:

Alkaloids Test:

Mayer Test: 2 mL of 1% Hydrochloric acid (HCl) was mixed with 0.5 mL of the leaf extract and gently heated, this mixture was treated with 1 mL of Mayer's reagent which resulted in the formation of precipitate with greenish or cream color indicating the presence of the alkaloids.

Dragendoff's Test: 2 mL of 1% Hydrochloric acid (HCl) was mixed with 0.5 mL of the leaf extract and gently heated to this mixture, drop by drop 1 mL of Dragendoff's reagent was added which resulted in the formation of precipitate with reddish-brown color indicating the presence of the alkaloids.

Wagner's Test: 2 mL of 1% Hydrochloric acid (HCl) was mixed with 0.5 mL of the leaf extract and gently heated, to this drop by drop 1 mL of Wagner's reagent was added resulting in the formation of precipitate with reddish-brown color showing the presence of the alkaloid.

Flavonoids Test:

Shinoda Test: A few fragments of Magnesium ribbon were mixed with the 2 mL of leaf extract and concentrated Hydrochloric acid was added drop wise. This resulted in the formation of a pink scarlet color after a few minutes indicating flavonoids' presence.

Test with Alkaline reagent: 2 mL of 2% NaOH solution was mixed with the 2 mL of the leaf extract which resulted in the formation of an intense yellow color further by the addition of a few drops of diluted acid turned colorless indicating the presence of flavonoids.

Test for Glycosides:

Keller-Kilani Test: 2 mL of glacial acetic acid having 1 to 2 drops of 2% Ferric chloride solution was mixed with 2 mL of leaf extract. This mixture was transferred into a new test tube having 2 mL of concentrated Sulfuric acid which resulted in the formation of a brown color ring indicating the glycosides' presence.

Steroids Test:

Liebermann-Burchard Test: 2 mL of each chloroform and acetic acid were mixed with 2 mL of the leaf extract and the mixture was ice-cooled, to this mixture concentrated sulfuric acid was added cautiously which shows the change in color from violet/blue to green/green-blue color indicating the presence of the steroid.

Test for phenolic compounds: A few mL of gelatin solution was added to 1 mL of the leaf extract resulting in the formation of a white color precipitate revealing the presence of the phenolic compounds. Lead tetra acetate was added to 1 mL of the leaf extract which resulted in the formation of precipitate showing the presence of the phenolic compounds.

Test for tannins: For the following tests, 15 mL of the leaf extract was taken and divided into 3 portions.

Test of Ferric Chloride: To the first test tube with crude leaf extract, three drops of $FeCl_3$ diluted solution were added which lead to the formation of greenish-black or blue color which further changed into olive green color upon addition of more $FeCl_3$ indicating the presence of tannins.

Test with Bromine Water: To the second test tube with crude leaf extract, 3 drops of bromine water was added which lead to the formation of a precipitate with buff color indicating the presence of condensed tannins and none was given for hydrolysable tannins.

Test with Lead sub-acetate: To the third test tube with the crude leaf extract, 3 drops of $Pb(C_2H_3O_2)_2$ was added which resulted in the formation of a colored precipitate suggesting tannins' presence.

Test for saponins: There were two methods followed to screen saponins.

Evaporated residue from the extract was dissolved in water. After vigorously shaking honeycomb froth persisted for 30 mins indicating the presence of saponins.

In another method 5 mL Chloroform was taken to dissolve the residue and filtered it. To this iced filtrate, concentrated sulfuric acid was added drop wise and also 1 mL acetic anhydride. This resulted in the formation of reddish brown or bluish green, blue color which often go along with the pink color ring formation showing the saponins presence.

Terpenoids Test:

Salkowski Test: 2 mL of chloroform was taken and mixed with 2 mL of the leaf extract and further 2 mL of sulfuric acid was added to it cautiously and gently shaken resulting in the formation of reddish-brown color indicating the presence of terpenoids.

Test for reducing sugars:

Fehling's test: Fehling reagents A and B together were mixed and 2 mL of this mixture was added to the 2 mL of leaf extract and boiled gently. At the bottom of the test tube a precipitate of brick-red color appeared which shows the reducing sugars' presence.

Benedict's test: When 2 mL of benedict's reagent was mixed with 2 mL of leaf extract and boiled, a precipitate of reddish-brown color was formed indicating the presence of carbohydrates.

Molisch's test: When 2 mL of Molisch's reagent was mixed with 2 mL of the leaf extract and this mixture was properly shaken, then 2 mL of Con. H_2SO_4 acid was added along the test tube's wall cautiously which results in the formation of a violet color ring at interphase indicating the carbohydrates' presence.

Test for protein and amino acids:

Millon's test: When 2mL of million's reagent was mixed with the 2 mL of leaf extract then a precipitate of the white color is formed which upon heating gently, turned into red color confirming the proteins' presence.

Ninhydrin test: When 2 mL of 0.2% ninhydrin solution was boiled with 2 mL of leaf extract then the color of violet appeared suggesting that proteins and amino acids were present.

Biuret test: 1 drop of 2% $CuSO_4$ (Copper sulfate) solution was used to treat 2 mL of leaf extract filtrate and added with excess KOH (Potassium Hydroxide) pellets and 1 mL ethanol which lead to the appearance of pink color in the ethanolic layer confirming the presence of the protein.

Test for fixed fats and oils: Between two filter papers, a drop of concentrated leaf extract was fused and set aside without disturbing it and the oil stain on the filter paper suggests the presence of fats and oils.

Test for Resins: 2 mL of acetic anhydride was taken to dissolve 2 mL of the leaf extract, to this mixture a drop of concentrated H_2SO_4 was added resulting in the formation of purple color which changed rapidly to a violet color indicating the presence of the resin.

Table.1. Phytochemical screening of Croton *bonplandianum L* leaf extract

Name of Phytoconstituents	Leaves	Name of Phytoconstituents	Leaves
Alkaloids	+	Saponins	+
Flavonoids	+	Terpenoids	+
Glycosides	+	Reducing Sugars	+
Steroids	+	Proteins and Aminoacids	+
Phenols	+	Fixed Oils and Fats	+
Tannins	+	Resins	+

+ is Present, - is Absence

Characterization: The formation of Ag-Cu BMNPs was confirmed by the following techniques. UV-Visible absorption spectral analysis using UV-2450 SHIMADZU double beam spectrophotometer in the wavelength ranged from 300-800 nm. Fourier Transform Infrared spectral analysis using Bruker Vector 22 spectrometer in the range of 4000-400 cm^{-1}. X-ray diffraction studies were recorded on a Rigaku Ultima IV X-ray diffractometer operated with Cu Kα source at a voltage of 40 kV and a current of 30 mA with a scan rate of 2.0 degrees per minute. FESEM, EDX studies were done by using Hitachi S-3700N machine with accelerating voltage 0.3-30 kV and magnification 5x - 300000x. Morphology of BMNPs was elucidated by HRTEM analysis with an FEI Technai machine operated at 300 kV. BET adsorption analysis is done with BELSORP MAX II instrument.

3. RESULTS AND DISCUSSION

UV-Visible spectral analysis: Visible absorption spectrum of Ag-Cu BMNPs is presented in Figure 5. The characteristic surface plasmon resonance (SPR) band at around 438 nm is observed in Ag-Cu BMNPs which confirms the nano size of the synthesized BMNPs.

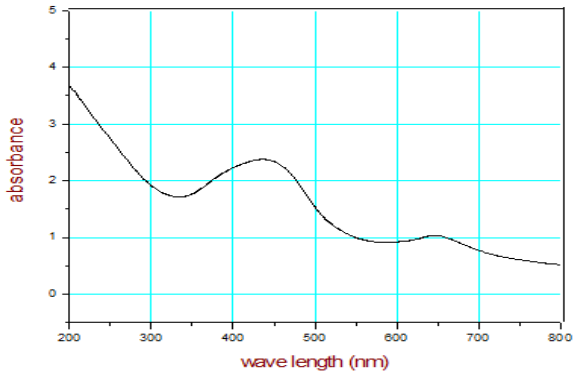

Figure.5. UV-Visible absorption spectrum of Ag-Cu BMNPs

FTIR spectroscopic analysis: FTIR spectral data is used to identify different functional groups present in biomolecules of leaf extract. These groups are responsible for the bio reduction of Ag^{+}, Cu^{+2} precursors and also for capping and stabilization of Ag-Cu BMNPs. The intense peaks were observed and compared with standard values to analyze the functional groups in *Croton bonplandianum* leaf extract and green synthesized Ag-Cu BMNPs. FTIR spectrum of synthesized Ag-Cu BMNPs by using *Croton bonplandianum* leaf extract were shown in Figure 6. The comparison of the FTIR spectra of both Ag-Cu BMNPs and leaf extract of *Croton bonplandianum* (Figure 7) clearly indicates the existence of the plant extract phytomolecules such as polyphenols, terpenes, flavonoids, glycosides, tannins, sterols, amides, carbohydrates, and amines on the surface of the Ag-Cu BMNPs.

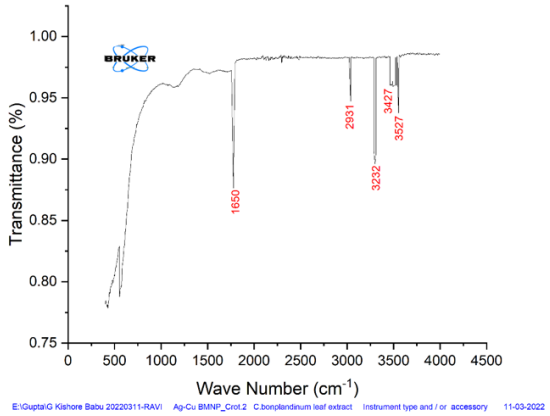

Figure.6. FTIR spectrum of Ag-Cu BMNPs

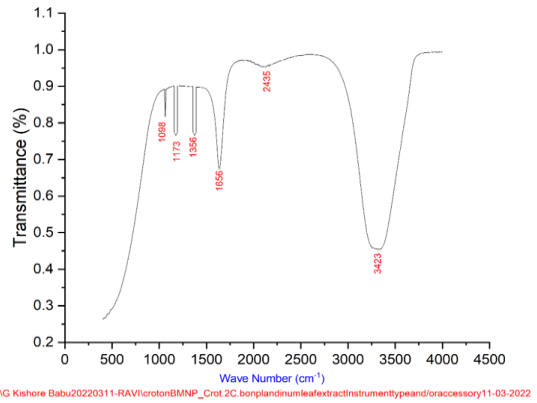

Figure.7. FTIR spectrum of *Croton bonplandianum L* leaf extract

The FTIR spectrum of Ag-Cu BMNPs exhibits major peak positions at 2931 cm^{-1}, 3232 cm^{-1}, 3427 cm^{-1}, and 3527 cm^{-1} which indicate the N-H stretching vibrations of amines and O-H stretching of hydroxyl groups of alcohols and phenols. An intense peak at 1650 $cm^{-1}$is due to C=O stretching of the amide group (Anita, 2018; Subramanian, 2019).

FTIR analysis clearly confirms that all the aforesaid absorption peaks of the extract are barely shifted in the FTIR spectrum of Ag-Cu BMNPs as the Phytomolecules of the extract act as bio reducing agents, capping and stabilizing agents for the synthesized nanoparticles. The existence of these IR bands also in the Ag-Cu BMNPs confirmed that the surface of the nanoparticles was covered by plant secondary metabolites such as carbohydrates, glycosides, Saponins, phytosterols, phenolic compounds, tannins, flavonoids, proteins, amino acids, diterpenes with functional group phenols, carboxylic acids, amides, ketones, alkyl halides (Suganya and Subasri, 2018).

FESEM micrographs and EDX analysis: From energy dispersive X-ray analysis we can analyze all the elements present in prepared BMNPs by *Croton bonplandinum L* leaf extract. Figure 8 and Table 2, shows the EDX spectrum and elemental composition of Ag-Cu BMNPs respectively. EDX study gives the quantitative data of silver and copper elemental compositions in the synthesized BMNPs**.** FESEM images of Ag-Cu BMNPs with various magnifications are given in Figure 9. From this, it can be clearly noted that the prepared Ag-Cu bimetallic nanomaterials are within the size range of 60 to 110 nm in diameter.

Table.2. Quantitative results of Ag-Cu BMNPs

Element	Weight %	Atomic %
Cu	55.69	66.70
Ag	31.82	29.45
O	12.49	3.85
Totals	100.00	100.00

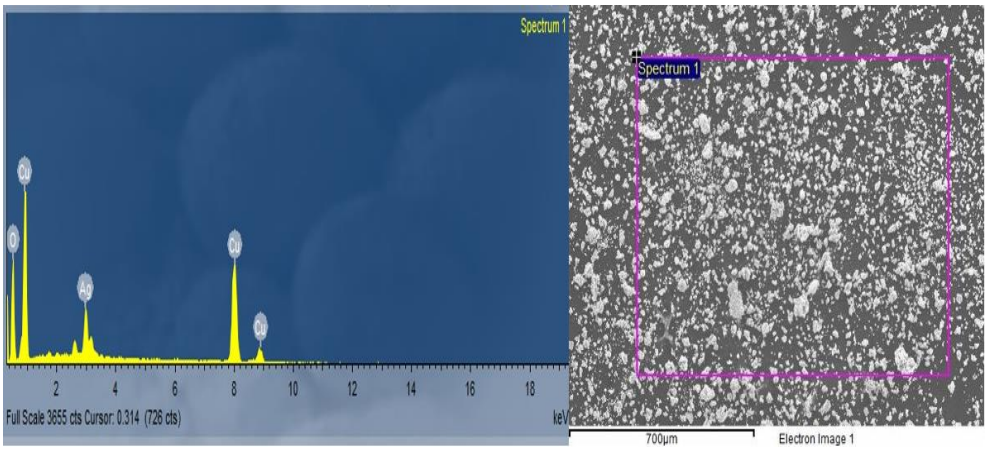

Figure.8. EDX analysis of Ag-Cu BMNPs

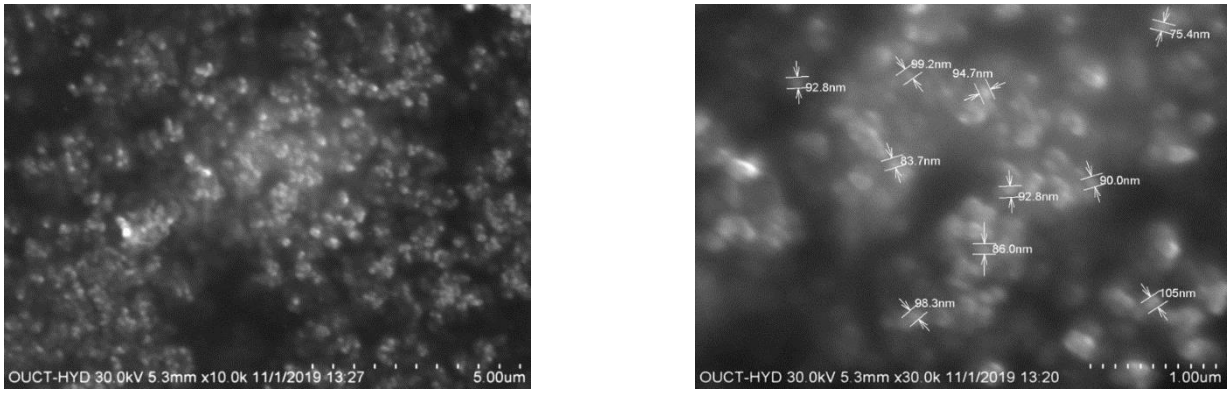

Figure.9. FESEM images of Ag-Cu BMNPs

HRTEM analysis: Figure 10, reveals the HRTEM images for synthesized Ag-Cu BMNPs from *Croton bonplandinum L leaf* extract. From these images, it was observed that Ag-Cu BMNPs were formed with spherical morphology and crystalline structure below 120 nm in size. More specifically, the two metal nanospheres seem to be positioned side by side, providing an overall bilobal structure. It is also in strong accordance with the images from the FESEM analysis.

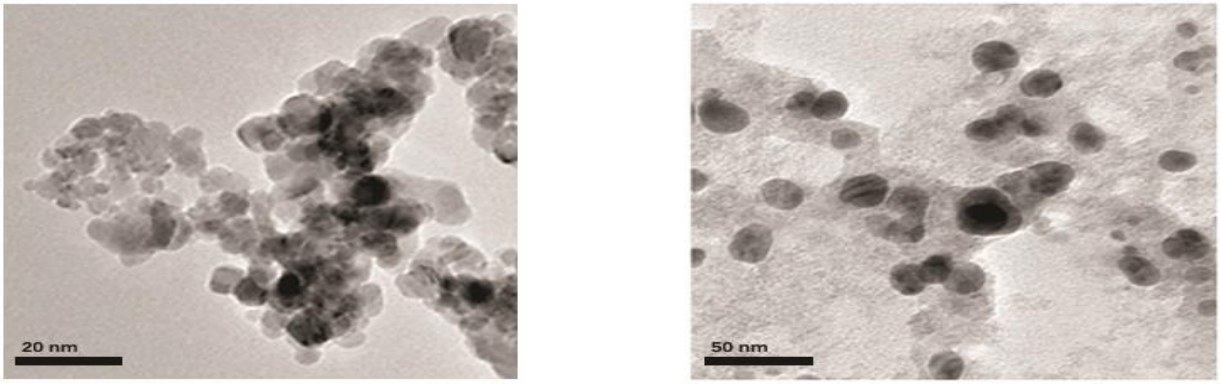

Figure.10. HRTEM images of Ag-Cu BMNPs

Powder XRD analysis: The XRD spectrum of green synthesized Ag-Cu BMNPs from leaf extract is shown in Figure 11. The peaks appeared at 2θ values of 36.84^0, 42.73^0, 61.77^0, 73.91^0 corresponding to Bragg's reflections of Ag (111), Ag (200), Cu (110), Ag (220), Cu (220), Ag (311) planes respectively of face-centered cubic crystal structure.

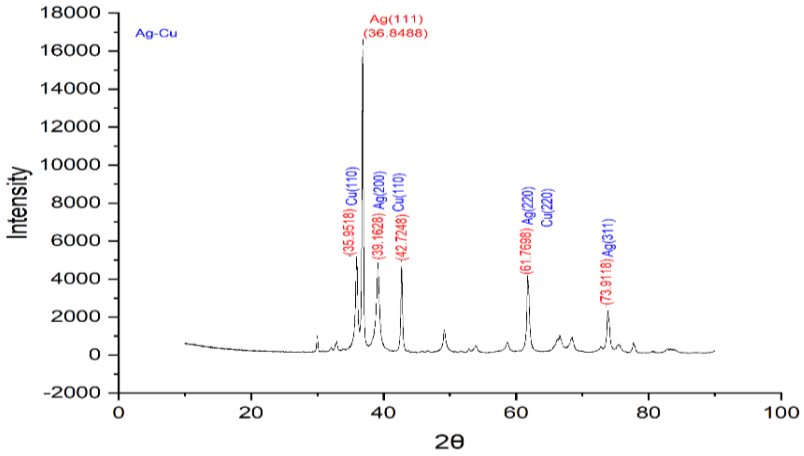

Figure.11. XRD spectrum of Ag-Cu BMNPs

The mean size D (in nm) of Ag-Cu bimetallic nanoparticles was computed by using the Debye-Scherrer equation

$$D=\frac{K\lambda}{\beta\cos\theta}$$

Where, D = crystalline size of Ag-Cu BMNPs; λ = wavelength of X-ray source (0.15406 nm) used in XRD; β = full width at half maximum (FWHM) of the diffraction peak; K = Scherrer constant = 0.9; θ = Bragg's angle.

Table.3. Crystalline sizes of Ag-Cu BMNPs

S.No.	2θ (degrees)	θ (radians)	Cos θ	B (radians)	D (nm)
1	36.84^0	0.6429	0.800361	0.005715	25.26323
2	42.73^0	0.7458	0.734545	0.004877	28.42796
3	61.77^0	1.0781	0.473003	0.003245	42.73111
4	73.91^0	1.2899	0.277217	0.001866	75.3186

The values of crystalline sizes for different 2θ values were calculated as per the Debye- Scherrer equation and given in Table 3. The numerically calculated value of the synthesized Ag-Cu BMNPs corresponds to an average particle size of 42.4352nm.

Photo-Catalytic Degradation:

Effect of time of contact: The efficiency of photo degradation of the Ag-Cu BMNPs on methylene blue dye was studied by batch mode experiments. The efficiency of BMNPs on the degradation of MB is expected to be increased by increasing contact time. The effect of contact time was carried out by taking 10 ppm of 100 ml MB dye solution and 10 mg of BMNPs (at pH 7) as catalyst load. The color change in dye solution was shown in Figure 12 and the corresponding plot was given in Figure 13. Initially, degradation of dye by using BMNPs was found to be rapid and then it almost settles down as a percentage of the degradation attains more or less constant value with this increase in contact time (Table 4). This is due to strong adsorption forces predominating between

the dye and the BMNPs and as the number of the reactive sites on the catalyst were vacant during initial periods of contact time. But after 120 minutes of contact time, percent degradation gradually approached a constant value to when equilibrium was almost reached because the number of vacant sites available for further dye adsorption is inevitably diminishing (Kah Aik Tan, 2012).

(1) - 0 mins; (2) - 30 mins; (3) - 60 mins; (4) - 90 mins; (5) - 120 mins; (6) - 150 mins; (7) - 180 mins

Figure.12. Color change in MB dye after addition of Ag-Cu BMNPs at various time intervals

Table.4. Contact time vs % photo degradation with Ag-Cu BMNPs

S.No.	Contact time (min)	% photo degradation
1	0	0
2	30	22.86
3	60	37.21
4	90	71.60
5	120	81.57
6	150	86.25
7	180	89.48

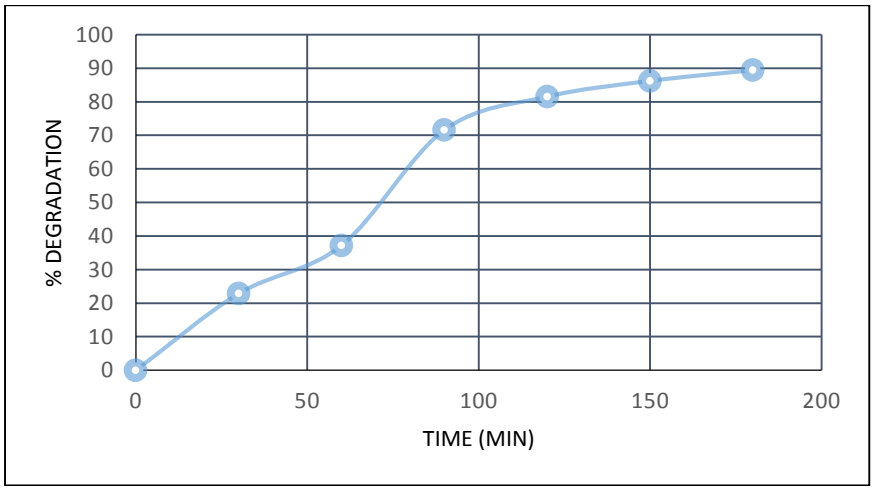

Figure.13. Effect of contact time on photo degradation

Effect of initial concentration of MB dye solution: The initial concentration of methylene blue (MB) dye solution is also expected to influence the rate of photo degradation. To investigate this fact, the dosage of BMNPs nano-catalyst was kept constant at 10 mg, keeping solution pH at 7 and the time of irradiation was maintained as 180 minutes. Whereas the initial concentrations of the MB dye solutions were varied at 5 ppm, 10 ppm, 15 ppm, 20 ppm, 25 ppm, 30 ppm and 35 ppm. The rate of photo degradation can be represented graphically in Figure 14 and results were given in Table 5. From the figure it can be observed that the highest degradation is located at 5 ppm, and the photo degradation decreases gradually with raise in the concentration of MB dye solution. This finding can be explained by the fact that as the concentration of the dye increases, the dye continues to act as a barrier for the incident radiation and does not allow the light intensity to touch the BMNPs surface and thus the % photo degradation decreases (Ameta, 2014).

Table.5. Concentration of dye vs % photo degradation with Ag-Cu BMNPs

S.No.	Concentration of dye solution (ppm)	% photo degradation
1	5	85.27
2	10	75.30
3	15	61.73
4	20	52.37
5	25	36.16
6	30	22.26
7	35	13.69

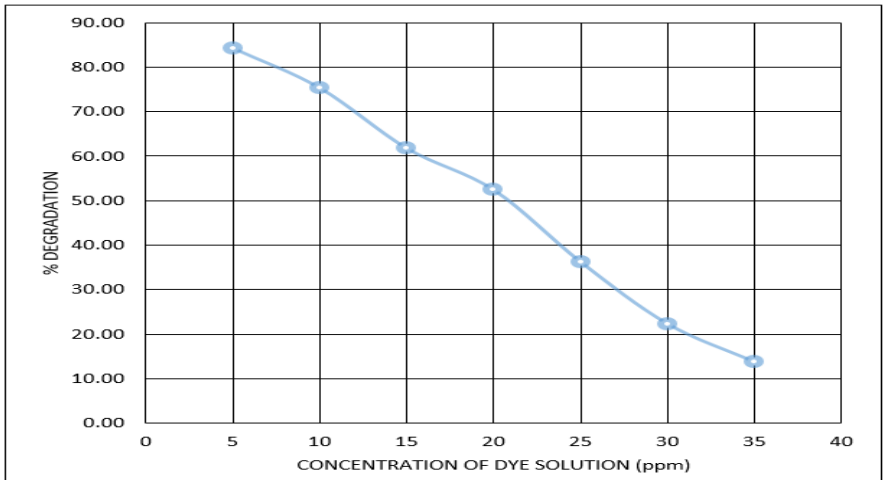

Figure.14. Effect of concentration of MB dye solution on photo degradation

Effect of pH: pH of dye solution can influence the adsorption of dye on photo catalyst. The initial concentration of methylene blue solution 10 ppm and the concentrations of the photo catalyst 10 mg were kept constant with time of irradiation 120 minutes. Different solutions of various pH values of 4 to 11 were prepared. Degradation efficiencies were compared which was given in Table 6 and shown in Figure 15.

Table.6. pH vs % photo catalytic degradation with Ag-Cu BMNPs

S.No.	pH of the solution	% photo degradation
1	4	47.15
2	5	53.03
3	6	63.33
4	7	70.97
5	8	86.68
6	9	85.67
7	10	76.07
8	11	68.36

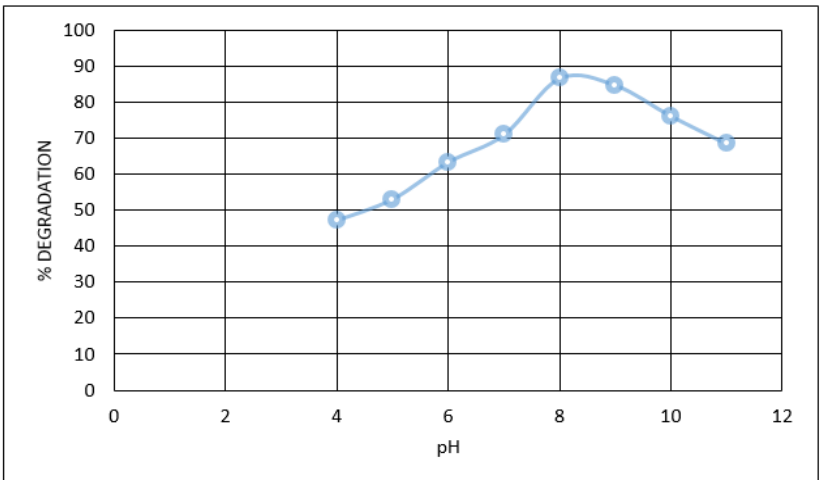

Figure.15. Effect of pH on photo degradation

It was noted that at initial pH values the degradation was minimum. So MB dye undergoes less degradation. Also in the acidic condition, the H^+ ions were made to compete with cationic MB dye, and hence the adsorption of dye was decreased. In contrast at pH > 9 in the more alkaline medium, the surface of the catalyst contains a huge number of OH^- ions that may proffer a negative charge to the adsorbent resulting in a great efficiency for the removal of MB dye (Xiulan Weng, 2014).

Effect of dosage of photo catalyst: In the photo catalytic degradation process, one of the important parameters of decolorizing of dye solution is photo catalyst dosage. To avoid unnecessary wastage of excessive catalysts and attain the maximum absorption of photons optimization of the catalyst dosage is essential. For this, the dosage amount was varied from 10 mg to 70 mg taken in 100 mL of 10 ppm MB dye at pH 8 with a contact time of 120 minutes. The % degradation of MB was given in Table 7 and the plot was shown in Figure 16.

Table.7. Catalyst dosage vs % photo degradation with Ag-Cu BMNPs

S.No.	Catalyst dosage (mg)	% photo degradation
1	10	83.99
2	20	86.67
3	30	95.31
4	40	86.92
5	50	83.99
6	60	78.57
7	70	72.25

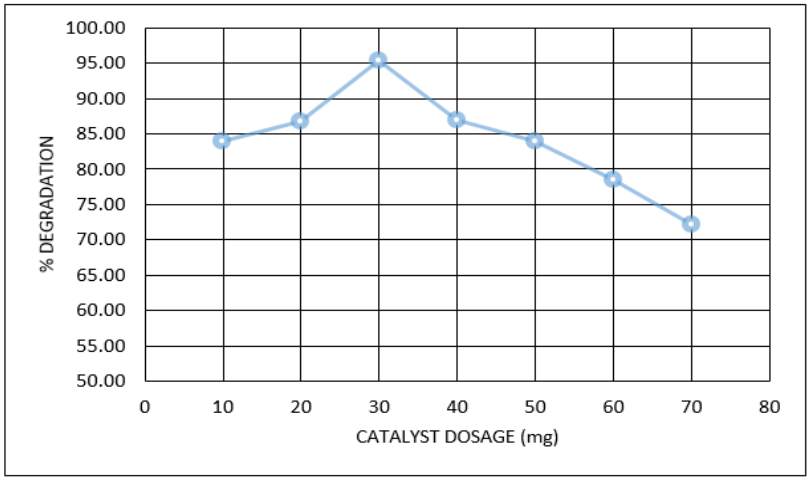

Figure.16. Effect of dosage of catalyst on photo degradation

It was concluded that by increasing the dosage of catalyst from 10 mg to 80 mg in 100 mL, the degradation of methylene blue dye enhances because the rise in the amount of catalyst up to 40 mg would increase the reactive sites that produce more reactive species. On further loading of catalyst, the percentage of degradation of methylene blue dye decreases. This can be rationalized by the fact that the addition of excess catalyst results in more turbid suspensions and decelerates the light penetration into the solution. Due to particle-particle interactions (agglomeration) and sedimentation of the catalyst, there will be a significant decrease in the active surface area and hence the degradation falls down (Hina Naeem, 2019).

Reusability of catalyst: The reusability of the green synthesized bimetallic Ag-Cu Nano catalyst was investigated by the repeated use of the catalyst, after each run, the catalyst was separated by centrifugation, washed with distilled water, and dried at 120^0C for 12 hours. The catalyst was efficient for two runs for MB degradation; however, the catalyst lost its efficiency at the third run for the same dye degradation. This may be due to the strong adsorption of dye blocking the active sites of the catalyst. Hence this catalyst could not be reused.

4. CONCLUSION

An ecologically safe method is projected in this report to synthesize Ag-Cu bimetallic nanoparticles from *Croton blanpondinum L* leaf extract. From UV-VIS spectral analysis it is confirmed that the particles are in nano scale as per the positions of the Surface Plasmon Resonance (SPR) bands. FTIR data confirms the presence of secondary metabolites of phyto-molecules that act as the bio reducing and capping agents of the formed nanoparticles. Results of XRD and SEM analyses proved that Ag-Cu BMNPs are in spherical morphology and cubic crystalline structure with size between 20-100 nm. The photo catalytic activity of these nanoparticles is examined under Sunlight for degradation of MB dye which is an environmental pollutant. The % of photo degradation of MB dye changes with parameters such as contact time, the concentration of MB dye, pH, photo

catalyst dosage. From this research study on bimetallic Ag-Cu BMNPs synthesized from *Croton blanpondinum L* leaf extract, the optimum conditions found in the degradation of MB dye is pH 8, the weight of catalyst 30 mg, dye concentration of 10 ppm and contact time of 180 minutes. A maximum photo degradation of ~ 85-89% could be obtained under these optimum conditions.

Conflicts of interest: We declare that we have no conflicts of interest.

5. ACKNOWLEDGEMENT

Authors profusely UGC-RGNF(F1-17.1/2016-17/RGNF-2015-17-SC-AND-9605/(SA-III)), for supporting financially throughout the work. Instrumentation help was provided by IIPE, Visakhapatnam, Pharmaceutical Sciences, Andhra University, Visakhapatnam.

B. Kishore babu and K. Mohana Rao acknowledges grants from the Ref No: 42-354/2013 UGC (India), New Delhi. We are grateful for the technical assistance provided by the Department of Engineering Chemistry at the Andhra University, Visakhapatnam (India) and the University of Hyderabad for providing the spectral data.

REFERENCES

Ameta K.L, Papnai N, and Ameta R, Synthesis, Characterization, and Use of Novel Bimetal Oxide Catalyst for Photo assisted Degradation of Malachite Green Dye, Journal of Materials, 2014, 1–5.

Anita A, Malar Retna A, Joseph J, Phytochemical screening and column chromatography studies of Aerva lanata, Asian Journal of Research in Chemistry, 11 (1), 2018, 84-90.

Chandel Anuj K, Silva Silvio S, Singh Om, Detoxification of Lignocellulosic Hydrolysates for Improved Bioethanol Production, Biofuel Production, 2011.

Daniel MC, Astruc D, Gold nanoparticles: assembly, supramolecular chemistry, quantum size-related properties, and applications toward biology, catalysis, and nanotechnology, Chemical Reviews, 104 (1), 2004, 293–346.

Divya B, Kenganora Mruthunjaya and Manjula S.N, Parkinsonia aculeata: A Phytopharmacological Review, Asian Journal of Plant Sciences, 10 (3), 2011, 175-181.

Greer JR, and Nix WD, Nanoscale gold pillars strengthened through dislocation starvation, Phys. Rev B, 73 (24), 2006.

Hina Naeem, Muhammad Ajmal, Raheela Beenish Qureshi, Sedra Tul Muntha, Muhammad Farooq, Muhammad Siddiq, Facile synthesis of graphene oxide–silver nanocomposite for decontamination of water from multiple pollutants by adsorption, catalysis and antibacterial activity, Journal of Environmental Management, 230, 2019, 199-211.

Jeeshna M.V, Paulsamy S, and Mallikadevi T, Phytochemical Constituents and Antimicrobial Studies of the Exotic Plant Species, *Croton bonplandianum* Baill, Journal of Life Sciences, 3 (1), 2011, 23-27.

Kaehler T, Nanotechnology: basic concepts and definitions, Clin. Chem., 40 (9), 1994, 1797–1799.

Kah Aik Tan, Norhashimah Morad, Tjoon Tow Teng, Ismail Norli, Panneerselvam P, Removal of Cationic Dye by Magnetic Nanoparticle (Fe_3O_4) Impregnated onto Activated Maize Cob Powder and Kinetic Study of Dye Waste Adsorption, APCBEE Procedia, 1, 2012, 83-89.

Koduru J.R, Kailasa S.K, Bhamore J.R, Kim K.H, Dutta T, and Vellingiri K, Phytochemical-assisted synthetic approaches for silver nanoparticles antimicrobial applications: A review, Advances in Colloid and Interface Science, 256, 2018, 326–339.

Lakshi Saikia, Diganta Bhuyan, Mrinal Saikia, Banajit Malakar, Dipak Kumar Dutta, Pinaki Sengupta, Photo catalytic performance of ZnO nanomaterials for self-sensitized degradation of malachite green dye under solar light, Applied Catalysis A: General, 490, 2015, 42-49.

Lee J, Park E.Y, and Lee J, Non-toxic nanoparticles from phytochemicals: preparation and biomedical application, Bioprocess and biosystems engineering, 37 (6), 2014, 983-989.

Maksakova O.V, Webster R.F, Tilley R.D, Ivashchenko V.I, Postolnyi B.O, Bondar O.V, and Pogrebnjak A.D, Nanoscale architecture of (CrN/ZrN)/(Cr/Zr) nanocomposite coatings: Microstructure, composition, mechanical properties and first-principles calculations, Journal of Alloys and Compounds, 2020, 154808.

Mansoori GA, Soelaiman TAF, Nanotechnology- an introduction for the standards community, Journal of ASTM International, 2 (6), 2005, 1-21.

Oyi A.R, Onaolapo J.A, and Obi R.C, Formulation and Antimicrobial Studies of Coconut (Cocos nucifera Linne) Oil, Research Journal of Applied Sciences, Engineering and Technology, 2 (2), 2010, 133-137.

Pantidos N, Biological Synthesis of Metallic Nanoparticles by Bacteria, Fungi and Plants, Journal of Nanomedicine & Nanotechnology, 5 (5), 2014.

Park Y, Hong Y.N, Weyers A, Kim Y.S, and Linhardt R.J, Polysaccharides and phytochemicals: a natural reservoir for the green synthesis of gold and silver nanoparticles, IET nano biotechnology, 5 (3), 2011, 69-78.

Parthiban A, Sivasankar R, Sachithanandam V, Ajmal Khan S, Jayshree A, Murugan K, Sridhar R, An integrative review on bioactive compounds from Indian mangroves for future drug discovery, South African Journal of Botany, 2021.

Ramamurthy CH, Padma M, samadanam DM, Mareeswaran R, Suyavaran A, Kumar MS, Premkumar K, Thirunavukkarasu C, The extra cellular synthesis of gold and silver nanoparticles and their free radical scavenging and antibacterial properties, Colloids Surf B Biointerfaces, 2013.

Ravindra Kumar Gautam, Vandani Rawat, Sushmita Banerjee, Maria Angeles Sanroman, Shivani Soni, Sanjeev K. Singh, Mahesh Chandra Chattopadhyaya, Synthesis of bimetallic Fe–Zn nanoparticles and its application towards adsorptive removal of carcinogenic dye malachite green and Congo red in water, Journal of Molecular Liquids, 212, 2015, 227-236.

Sahoo A, Singh B, Bhat T.K, Effect of tannins on *in vitro* ruminal protein degradability of various tree forages, Livestock Research for Rural Development, 22 (7), 2010.

Selvamangai G and Bhaskar Anusha, GC–MS analysis of phytocomponents in the methanolic extract of Eupatorium triplinerve, Asian Pacific Journal of Tropical Biomedicine, 2 (3), 2012, S1329–S1332.

Shah M, Fawcett D, Sharma S, Tripathy S.K, and Poinern G.E.J, Green synthesis of metallic nanoparticles via biological entities, Materials, 8 (11), 2015, 7278-7308.

Sirdeshpande K.D, Sridhar A, Cholkar K.M, and Selvaraj R, Structural characterization of mesoporous magnetite nanoparticles synthesized using the leaf extract of *Calliandra haematocephala* and their photocatalytic degradation of malachite green dye, Applied Nanoscience, 8 (4), 2018, 675–683.

Srinoi P, Chen Y.T, Vittur V, Marquez M.D, and Lee T.R, Bimetallic Nanoparticles: Enhanced Magnetic and Optical Properties for Emerging Biological Applications, Applied Science, 8 (7), 2018, 1106.

Subramanian A, Raman N, and Dhasarathan P, Study on antibacterial activity of phytochemicals obtained from Aerva lanata, Asian Journal of Pharmacy and Pharmacology, 5 (4), 2019, 721-727.

Suganya R, and Subasri G, Phytochemical characterization and evaluation of the antimicrobial activity of Aerva lanata L, World Journal of Science and Research, 3 (1), 2018, 23-29.

Venkatesan P, and Santhanalakshmi J, Core-Shell Bimetallic Au-Pd Nanoparticles: Synthesis, Structure, Optical and Catalytic Properties, Nanoscience and Nanotechnology, 1 (2), 2011, 43–47.

Xiulan Weng, Lanlan Huang, Zuliang Chen, Mallavarapu Megharaj, Ravendra Naidu, Synthesis of iron-based nanoparticles by green tea extract and their degradation of malachite, Industrial Crops and Products, 51, 2014, 342-347.